SCIENTIFIC REPORTS

OPEN

High Temperature Terahertz Detectors Realized by a GaN High Electron Mobility Transistor

H. W. Hou[1,2], Z. Liu[1], J. H. Teng[3], T. Palacios[4] & S. J. Chua[1,2]

In this work, a high temperature THz detector based on a GaN high electron mobility transistor (HEMT) with nano antenna structures was fabricated and demonstrated to be able to work up to 200 °C. The THz responsivity and noise equivalent power (NEP) of the device were characterized at 0.14 THz radiation over a wide temperature range from room temperature to 200 °C. A high responsivity R_v of 15.5 and 2.7 kV/W and a low NEP of 0.58 and 10 pW/Hz$^{0.5}$ were obtained at room temperature and 200 °C, respectively. The advantages of the GaN HEMT over other types of field effect transistors for high temperature terahertz detection are discussed. The physical mechanisms responsible for the temperature dependence of the responsivity and NEP of the GaN HEMT are also analyzed thoroughly.

With the development of terahertz (THz) technologies, a compact, high speed, and highly sensitive detector working at sub-THz and THz ranges is highly desirable[1–6]. Field-effect transistors (FETs) have been used to fabricate THz detectors, benefiting from the nonlinear properties of the plasmonic excitations in the two-dimensional electron channels. Field-effect transistor THz detectors hold the advantages of high sensitivity, fast response, ability to operate at room temperature[7]. Different types of FETs, such as silicon metal-oxide-semiconductor FETs (MOSFETs), GaAs high electron mobility transistors (HEMTs), InP HEMTs, or GaN HEMTs have been reported with broadband responsivities for THz radiation[8]. For example, the responsivity of Si-FET integrated with a bow-tie antenna has reached 5 kV/W at 0.292 THz[9]. A very high responsivity of 22.7 kV/W at 0.2 THz has been demonstrated using an InP HEMT with an asymmetric dual-grating-gate[7]. GaN HEMTs integrated with a nano-antenna have shown a room temperature responsivity of 15 kV/W at 0.14 THz in our previous work[10].

It is demanding to develop terahertz detectors with high sensitivity at elevated temperatures for applications in a harsh environment. The currently widely used terahertz detectors are the bolometer, the pyroelectric detector, the Schottky diode, and Golay cells. Bolometers only work well at low temperatures. The pyroelectric detector and Golay cells detect terahertz radiation up to room temperature[11]. This is due to their intrinsic limitation that detection is based on the induced temperature change by the absorption of terahertz photons and a higher temperature will increase the background noise and reduce sensitivity. Schottky diode or FET detectors made of Si, GaAs, or InP have different detection mechanisms and are able to work at room temperature. However, Si, GaAs, or InP has a relatively narrow band gap (1.12~1.42 eV), and thereby a high intrinsic carrier density that increases exponentially with temperature, which will enlarge the device leakage current and degrade the device performance. Therefore, it is difficult for Si, GaAs, or InP FET terahertz detectors to work at high temperatures.

As a wide-bandgap material, GaN has attracted much interest from both academia and industry for electronic[12] and optoelectronic device applications[13]. GaN HEMTs have also shown excellent performance for sub-THz and THz detection. Panasonic Corp. has reported a detection responsivity of 1.1 kV/W at 1 THz using a GaN HEMT with 80 nm gate dipole antennas[14]. With a large bandgap of GaN at ~3.4 eV and thus lower intrinsic carrier density, GaN HEMTs are endowed with the potential to work well at high temperatures[15].

In this paper, we report for the first time a THz detector based on GaN HEMT with the ability to work at high temperatures up to 200 °C. It is the first semiconductor device allowing terahertz detection that can operate at

[1]Low-energy electronic system IRG, Singapore-MIT Alliance for Research and Technology Center, 1 CREATE Way, 138602, Singapore. [2]Department of Electrical and Computer Engineering, National University of Singapore, Block E4, Engineering Drive 3, 117583, Singapore. [3]Institute of Materials Research and Engineering, Agency for Science, Technology, and Research (A*STAR), 2 Fusionopolis Way, Innovis, 138634, Singapore. [4]Department of Electrical Engineering and Computer Science, Massachusetts Institute of Technology, 77 Massachusetts Avenue, Cambridge, Massachusetts, 02139, United States. Correspondence and requests for materials should be addressed to S.J.C. (email: elecsj@nus.edu.sg)

1

such a high temperature. The mechanisms inside the temperature dependence of the detection responsivity and the noise equivalent power (NEP) are also studied.

Advantages of GaN HEMTs for High Temperature Terahertz Detection

A fundamental theoretical description of the non-resonant THz detection in FETs has been given in the framework of the Dyakonov–Shur theory[16]. The induced terahertz detection signal ΔU can be found from

$$\Delta U = \frac{e}{m}\frac{U_a^2}{4s^2} \tag{1}$$

where s is the plasma wave velocity. The plasma wave velocity s is given by[17]

$$s^2 = \frac{e}{m}\frac{n}{dn/dU}\bigg|_{U=V_0} \tag{2}$$

By adding intrinsic carrier density n_i to the unified charge control model[18], the electron density n in the 2DEG channel of a HEMT can be described by:

$$n = \frac{C\eta k_B T}{e^2}\ln\left[1 + \exp\left(\frac{eV_0}{\eta k_B T}\right)\right] + n_i \tag{3}$$

Here, V_0 is the gate-to-channel voltage swing defined as $V_0 = V_g - V_{th}$, $C = en_0/$, V_{th} is the gate capacitance, η is the ideality factor, k_B is the Boltzmann constant, T is the absolute temperature, and n_i is the intrinsic carrier density of the semiconductor.

The intrinsic carrier density n_i of semiconductors can be determined by[19]:

$$n_i = \sqrt{N_c N_v}\exp\left(\frac{-E_g}{2k_B T}\right) \tag{4}$$

It can be seen that the intrinsic carrier density is exponentially dependent on the bandgap, which is a huge difference for semiconductors. N_c and N_v are the effective density of states in the conduction band and the valence band. In a bulk semiconductor, N_c and N_v are proportional to $T^{3/2}$. In a 2DEG system, as the energy level s are quantized and most of the electrons (more than 80%) occupy the first level[20], the influence of the temperature on N_c and N_v is very weak. Considering that the THz detection performance of a HEMT is much higher when it is operating in 2DEG depletion region than in accumulation region, we use 3D bulk temperature dependence for N_c which is approximately proportional to $T^{3/2}$, instead of the 2D temperature dependence.

The intrinsic carrier density for silicon is about $\sim 1 \times 10^{10}\,\mathrm{cm^{-3}}$. For GaAs, it is about $\sim 2 \times 10^6\,\mathrm{cm^{-3}}$, while for InP, it is about $1 \times 10^7\,\mathrm{cm^{-3}}$. However, for GaN, the intrinsic carrier density is extremely low ($\sim 1.9 \times 10^{-10}\,\mathrm{cm^{-3}}$) due to its wide bandgap, which will provide GaN unique properties for high temperature terahertz detection.

The temperature dependence of the band gap is calculated by the Varshni equation. Using Eqs (2) and (3), we get

$$s^2 = \left(\frac{\eta k_B T}{m}\ln\left[1 + \exp\left(\frac{eV_0}{\eta k_B T}\right)\right] + \frac{eV_{th}}{m}\left(\frac{n_i}{n_0}\right)\right)\left[1 + \exp\left(-\frac{eV_0}{\eta k_B T}\right)\right] \tag{5}$$

Combining Eqs (1) and (5), the terahertz response ΔU can be expressed as

$$\Delta U = \frac{U_a^2}{4}\frac{1}{\left(V_T\ln\left[1 + \exp\left(\frac{V_0}{V_T}\right)\right] + V_{th}\left(\frac{n_i}{n_0}\right)\right)\left[1 + \exp\left(-\frac{V_0}{V_T}\right)\right]} \tag{6}$$

where $V_T = \eta k_B T/e$ and is related to the sub-threshold slope; n_0 is the electron density in the channel (which is $1 \times 10^{13}\,\mathrm{cm^{-2}}$ for GaN HEMTs, $7 \times 10^{11}\,\mathrm{cm^{-2}}$ for GaAs HEMTs[21], $1 \times 10^{13}\,\mathrm{cm^{-2}}$ for InP HEMTs[22], and $3.5 \times 10^{11}\,\mathrm{cm^{-2}}$ for silicon MOSFET[3]); and U_a is the coupling efficiency of the incoming radiation to the antenna.

The normalized response degradation $(\Delta U(T) - \Delta U(300\,\mathrm{K}))/\Delta U(300\,\mathrm{K})$ with temperature for GaN HEMTs, GaAs HEMTs, InP HEMTs, and silicon MOSFETs is plotted in Fig. 1. At room temperature, the intrinsic carrier concentration is negligible compared to n_0 and the ratio $n_i/n_0 \ll 1$ for all the transistors. Therefore, the term $V_{th}(n_i/n_0)$ is negligible and Eq. (6) is reduced to the well-established equation used at room temperature[17]. In a low temperature region, all types of transistors decrease with T^{-1}, which is mainly a result of the V_T increment. When the temperature $> 100\,°\mathrm{C}$, the intrinsic carrier concentration n_i in silicon MOSFETs starts to influence the device performance so that the response degradation for silicon MOSFET reduces faster than in other type of FETs. As the temperature increases, the degradation of GaAs HEMTs and InP HEMTs speed up as well. It can be seen GaN HEMTs perform the best over other transistors, even up to $1000\,°\mathrm{C}$. At $1000\,°\mathrm{C}$, the intrinsic carrier concentration in GaN is only $3.86 \times 10^9\,\mathrm{cm^{-2}}$. It is still much lower than the channel concentration of $1 \times 10^{13}\,\mathrm{cm^{-2}}$, which indicates that the intrinsic carrier concentration little influence on GaN HEMTs. Another important finding is that the ultra-low intrinsic carrier concentration of GaN due to its $3.4\,\mathrm{eV}$ wide bandgap and its high channel carrier concentration of $1 \times 10^{13}\,\mathrm{cm^{-2}}$ make GaN HEMTs suitable for high temperature terahertz detection.
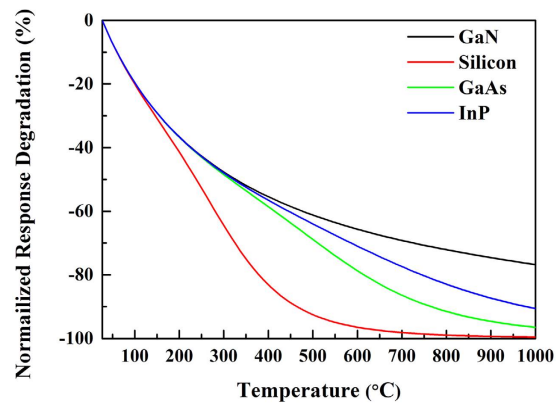
Figure 1. The normalized response degradation $(\Delta U(\mathrm{T}) - \Delta U(300\,\mathrm{K}))/\Delta U(300\,\mathrm{K})$ with temperature for GaN HEMTs, GaAs HEMTs, InP HEMTs and Silicon MOSFET.
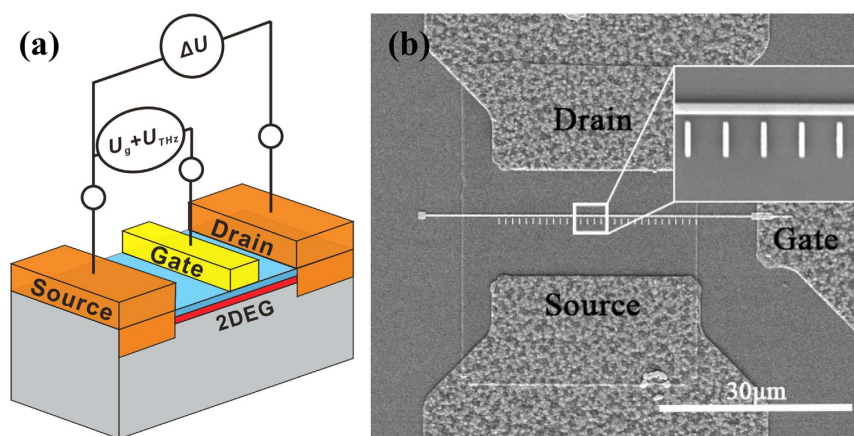
Figure 2. (**a**) The schematic diagram of GaN HEMT terahertz detector. (**b**) SEM image of the GaN HEMT terahertz detector from top view.

Another advantage of GaN HEMTs is their low subthreshold leakage at high temperature[23]. The subthreshold leakage is able to induce shot noise ($N_{shot} = (2eI_{leakge})^{0.5}$) for the terahertz detector. The wide band gap helps to suppress subthreshold leakage for the GaN terahertz detector.

## Demonstration of High Temperature GaN Terahertz Detector

The detector schematic is as shown in Fig. 2(a). The device fabricated is based on an $Al_{0.25}Ga_{0.75}N$/GaN heterostructure. The epilayers include a 3 nm unintentionally-doped (UID) GaN cap, a 20 nm UID $Al_{0.25}Ga_{0.75}N$ barrier, a 1 nm AlN spacer, a 1.5 μm GaN buffer layer, and transition/seeding layers. The epilayers were grown on a 6-inch high-resistivity Si(111) substrate. The typical 2-dimensional electron gas (2DEG) mobility and density are ~2100 cm²/Vs and ~1.0×10^{13} cm^{-2}, respectively, as measured by the Hall measurement.

The scanning electron microscopy (SEM) image of the top view of the THz detector is shown in Fig. 2(b). An asymmetric nano antenna was placed near the gate of the HEMT. The gate length is 250 nm and the nano antenna has the dimension of 100 nm × 1 μm. The gap between the gate and the nano antenna is 200 nm. The source-drain distance is 14 μm. The nano-antenna was designed to improve the coupling between the incident THz radiation and the plasmons in the 2DEG channel[10].

The transfer current-voltage characteristics were measured from room temperature to 200 °C, and they are shown in Fig. 3(a). The fabricated GaN devices exhibit good gate modulation and transfer properties. It can be seen that source-drain current decreases from 31 mA/mm at 30 °C to 17 mA/mm at 200 °C with $V_g = 0$ V and $V_d = 1$ V. This is mainly due to the mobility degradation at high temperature[20]. When the temperature is more than -173 °C, the 2DEG channel mobility is predominantly limited by the optical phonon scattering[24]. In addition, at higher temperature, the transconductance G_m is reduced, the curve of G_m versus V_g is broadened, and the G_m peak position is shifted. The broadening is due to the change of the thermal voltage V_T, which has its relationship with temperature as shown in Fig. 3(b), and to the ideal factorη[18]. The threshold voltage V_{th} is -4.5 V at room temperature and it shifts to a more negative voltage of -5.5 V at 200 °C, which is a typical behavior for the GaN HEMT[25].
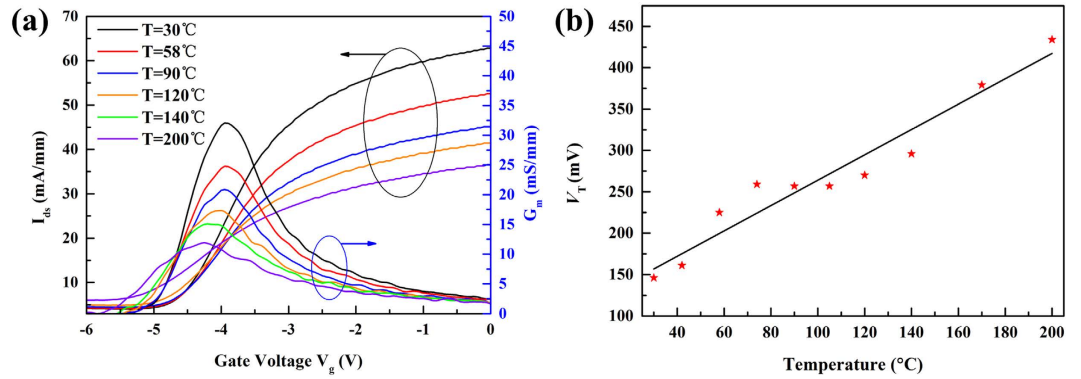
Figure 3. (**a**) The transfer characteristics of the GaN HEMT. (**b**) Temperature dependent modified thermal voltage V_T, obtained from transfer characteristics measurements.
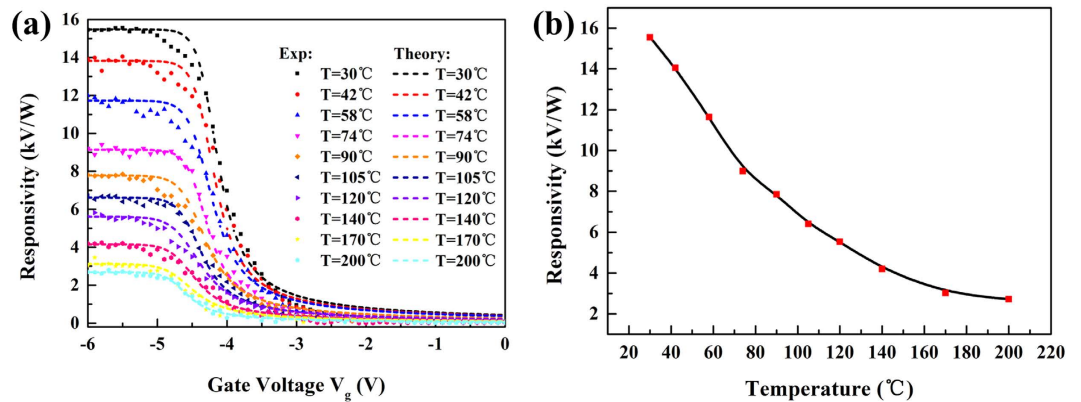
Figure 4. (**a**) Responsivity measured as a function of gate voltage at different temperatures for radiation at 0.14 THz. (**b**) Temperature dependent responsivity at $V_g = -5.5$ V.

The responsivity R_v as a function of the gate voltage (V_g) at different temperatures from room temperature to 200 °C is plotted in Fig 4(a). The sigmoid shapes of the responsivity versus gate bias are similar at all measured temperatures up to 200 °C. R_v starts to decrease when $V_g > V_{th}$, and it is close to zero when $V_g >> V_{th}$. When V_g decreases and enters the depletion regime ($V_g = -3$ to -5 V, around V_{th}), R_v starts to increase and saturates after the 2DEG channel is fully depleted ($V_g < V_{th}$).

As seen from Fig. 4(a), the responsivity decreases with the increase of temperature at all gate biases. The measured maximum responsivity at 0.14 THz was around 15 kV/W at room temperature, and it decreased by five times to 2.7 kV/W at 200 °C, as shown in Fig. 4(b). This decrease shows the excellent performance of the GaN HEMT to work as a THz detector at high temperatures. In addition, the position of the maximum THz responsivity negatively shifted as the temperature increased. This shift is due to the threshold voltage shift of the GaN HEMT, which is a typical behavior of a GaN HEMT[25].

Without the influence of an intrinsic carrier, the term determining the maximum THz response for GaN HEMTs mainly includes the modified thermal voltage V_T. As for the term V_T, due to the temperature dependence of η, the relationship between V_T and temperature T is not linear. The temperature dependence of V_T can be seen from the sub-threshold slope of the transfer characteristics of the GaN HEMT[26]. By analyzing the experimental transfer characteristics (Fig. 3(a)), the temperature dependence of V_T for our investigated transistor can be determined and plotted as shown in Fig. 3(b). It can be seen that the subthreshold slope decreases and the V_T increases with increasing temperature. According to Eq. (6), the detected voltage ΔU is inversely proportional to V_T, so it will become smaller at a higher temperature.

Noise equivalent power is an important figure of merit for a THz detector. The dominant noise source in the GaN terahertz detector is the thermal noise from the GaN channel. Therefore, the NEP can be estimated by Eq. (7):

$$NEP = (4k_B T R_{ds})^{0.5}/R_v \tag{7}$$

where R_{ds} is the channel resistance. R_{ds} can be determined from the static transfer characteristic shown in Fig. 3(a). Figure 5 shows the NEP value as a function of gate voltage from room temperature to 200 °C. Because of the additional factor R_{ds} in Eq. (7), the shape of the NEP versus the gate voltage does not follow that of R_v. Due to the sharp
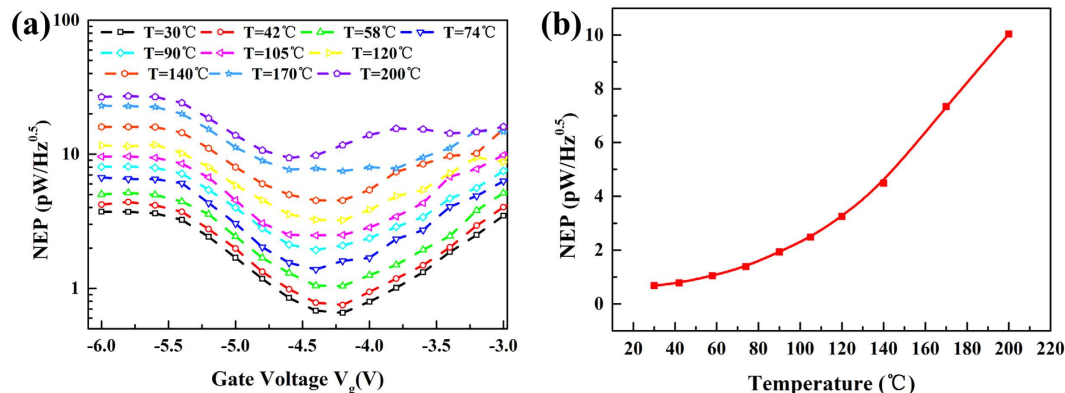
Figure 5. (**a**) NEP of the GaN HEMT detector as a function of gate voltage at different temperatures. (**b**) NEP of the GaN HEMT detector as a function of temperature at gate voltage $V_g = -4.4$ V.

rise of the channel resistivity, the NEP curve at $V_g < V_{th}$ shows a valley as indicated in Fig. 5(a). The increase of temperature leads to the increase of the thermal noise and thus the NEP. A minimal NEP value of 0.58 pW/Hz$^{0.5}$ is obtained at $V_g = -4.2$ V at room temperature, and 9.38 pW/Hz$^{0.5}$ is obtained at $V_g = -4.6$ V at 200 °C. Fig. 5(b) shows the temperature dependence of the NEP at the fixed gate voltage $V_g = -4.4$ V. Compared with the degradation of the responsivity R_v at high temperatures, the physical mechanisms inside the degradation of the NEP include an extra factor of thermal noise, which is proportional to $T^{0.5}$. To achieve higher operation temperature, surface states of GaN HEMTs can be passivated to enhance device thermal stability[27,28].

Conclusion

In conclusion, a THz detector working up to 200 °C was successfully demonstrated based on a nano-antenna GaN HEMT. A maximum responsivity 15 kV/W and 2.7 kV/W and a minimum NEP of 0.58 pW/Hz$^{0.5}$ and 9.38 pW/Hz$^{0.5}$ were achieved at 0.14 THz radiation at room temperature and 200 °C, respectively. The low intrinsic carrier concentration, high channel carrier concentration, and low subthreshold leakage were found to be advantages of the GaN terahertz detector at high temperatures. The excellent performance of the GaN THz detector manifests itself as a promising candidate for high temperature THz applications.

Methods

Device Fabrication. The fabrication process started from mesa patterning and isolation by Cl_2 based plasma etching. Source and drain ohmic contacts were formed with Ti/Al/Ni/Au (20/120/40/50 nm) by e-beam evaporation followed by 850 °C annealing in an N_2 atmosphere. The gate was realized by Ni/Au (20/80 nm) metallization. The surface was not passivated.

Experimental Setup. A 0.14 THz (full name) IMPATT diode was used as a continuous-wave (CW) sub-THz source with the output power of 0.1 mW, which was calibrated by a standard pyroelectric power meter. The THz radiation was focused onto the surface of the device with a beam spot size of around 1.5 mm in diameter by two off-axis parabolic mirrors. The drain terminal of the HEMT was not biased, and the gate terminal was biased through a DC power source (GWInstek GPD-3303S). The photovoltages ΔU generated at the drain-source terminal were read out by a SR830 lock-in amplifier. A 10 mm × 10 mm metal ceramic heater was attached on the backside of the device and a thermocouple was placed on the front side of the device to measure the device temperature. The responsivity R_v is defined as $\Delta U/P_d$, where ΔU is the measured photovoltage and P_d is the radiation power on the detector.

References

1. Ojefors, E., Pfeiffer, U. R., Lisauskas, A. & Roskos, H. G. A 0.65 THz Focal-Plane Array in a Quarter-Micron CMOS Process Technology. *Solid-State Circuits, IEEE Journal of* **44,** 1968–1976, doi: 10.1109/JSSC.2009.2021911 (2009).
2. Watanabe, T. *et al.* InP- and GaAs-Based Plasmonic High-Electron-Mobility Transistors for Room-Temperature Ultrahigh-Sensitive Terahertz Sensing and Imaging. *Sensors Journal, IEEE* **13,** 89–99, doi: 10.1109/JSEN.2012.2225831 (2013).
3. Lisauskas, A. *et al.* Rational design of high-responsivity detectors of terahertz radiation based on distributed self-mixing in silicon field-effect transistors. *Journal of Applied Physics* **105,** 114511; doi: http://dx.doi.org/10.1063/1.3140611 (2009).
4. Drexler, C. *et al.* Helicity sensitive terahertz radiation detection by field effect transistors. *Journal of Applied Physics* **111,** 124504, doi: http://dx.doi.org/10.1063/1.4729043 (2012).
5. Sakowicz, M. *et al.* Polarization sensitive detection of 100 GHz radiation by high mobility field-effect transistors. *Journal of Applied Physics* **104,** 024519, doi: http://dx.doi.org/10.1063/1.2957065 (2008).
6. Blin, S. *et al.* Plasma-Wave Detectors for Terahertz Wireless Communication. *Electron Device Letters, IEEE* **33,** 1354–1356, doi: 10.1109/LED.2012.2210022 (2012).
7. Kurita, Y. *et al.* Ultrahigh sensitive sub-terahertz detection by InP-based asymmetric dual-grating-gate high-electron-mobility transistors and their broadband characteristics. *Applied Physics Letters* **104,** 251114, doi: http://dx.doi.org/10.1063/1.4885499 (2014).
8. Knap, W. *et al.* Field Effect Transistors for Terahertz Detection: Physics and First Imaging Applications. *Journal of Infrared, Millimeter, and Terahertz Waves* **30,** 1319–1337, doi: 10.1007/s10762-009-9564-9 (2009).
9. Schuster, F. *et al.* Broadband terahertz imaging with highly sensitive silicon CMOS detectors. *Optics express* **19,** 7827–7832, doi: 10.1364/OE.19.007827 (2011).

10. Haowen, H., Zhihong, L., Jinghua, T., Tomás, P. & Soo-Jin, C. A sub-terahertz broadband detector based on a GaN high-electron-mobility transistor with nanoantennas. *Applied Physics Express* **10,** 014101 (2017).
11. Tonouchi, M. Cutting-edge terahertz technology. *Nat Photon* **1,** 97–105, doi: 10.1038/nphoton.2007.3 (2007).
12. Mishra, U. K., Parikh, P. & Yi-Feng, W. AlGaN/GaN HEMTs-an overview of device operation and applications. *Proceedings of the IEEE* **90,** 1022–1031, doi: 10.1109/JPROC.2002.1021567 (2002).
13. Nakamura, S., Pearton, S. & Fasol, G. *The blue laser diode: the complete story* (Springer Science & Business Media), doi: 10.1007/978-3-662-04156-7 (2013).
14. Tanigawa, T., Onishi, T., Takigawa, S. & Otsuji, T. In *Device Research Conference* (*DRC*), 167–168, doi: 10.1109/DRC.2010.5551895 (2010).
15. Medjdoub, F. *et al.* In *2006 International Electron Devices Meeting.* 1–4, doi: 10.1109/IEDM.2006.346935 (2006).
16. Dyakonov, M. & Shur, M. Detection, mixing, and frequency multiplication of terahertz radiation by two-dimensional electronic fluid. *IEEE Transactions on Electron Devices* **43,** 380–387, doi: 10.1109/16.485650 (1996).
17. Knap, W. *et al.* Nonresonant detection of terahertz radiation in field effect transistors. *Journal of Applied Physics* **91,** 9346–9353, doi: http://dx.doi.org/10.1063/1.1468257 (2002).
18. Shur, M., Fjeldly, T. A., Ytterdal, T. & Lee, K. Unified MOSFET model. *Solid-State Electronics* **35,** 1795–1802, doi: http://dx.doi.org/10.1016/0038-1101(92)90263-C (1992).
19. Sze, Simon M. & Kwok, K. Ng. *Physics of semiconductor devices* John wiley & sons, doi: 10.1002/0470068329 (2006).
20. Liu, Z. H., Arulkumaran, S. & Ng, G. I. Temperature dependence of Ohmic contact characteristics in AlGaN/GaN high electron mobility transistors from −50 to 200 °C. *Applied Physics Letters* **94,** 142105, doi: http://dx.doi.org/10.1063/1.3114422 (2009).
21. Preu, S. *et al.* Ultra-fast transistor-based detectors for precise timing of near infrared and THz signals. *Optics express* **21,** 17941–17950, doi: 10.1364/OE.21.017941 (2013).
22. Kurita, Y. *et al.* Ultrahigh sensitive sub-terahertz detection by InP-based asymmetric dual-grating-gate high-electron-mobility transistors and their broadband characteristics. *Applied Physics Letters* **104,** 251114, doi: 10.1063/1.4885499 (2014).
23. Neudeck, P. G., Okojie, R. S. & Liang-Yu, C. High-temperature electronics - a role for wide bandgap semiconductors? *Proceedings of the IEEE* **90,** 1065–1076, doi: 10.1109/JPROC.2002.1021571 (2002).
24. Dang, X. Z. *et al.* Measurement of drift mobility in AlGaN/GaN heterostructure field-effect transistor. *Applied Physics Letters* **74,** 3890–3892, doi: http://dx.doi.org/10.1063/1.124214 (1999).
25. Gaska, R. *et al.* High-temperature performance of AlGaN/GaN HFETs on SiC substrates. *Electron Device Letters, IEEE* **18,** 492–494, doi: 10.1109/55.624930 (1997).
26. Klimenko, O. A. *et al.* Temperature enhancement of terahertz responsivity of plasma field effect transistors. *Journal of Applied Physics* **112,** 014506, doi: http://dx.doi.org/10.1063/1.4733465 (2012).
27. Zhang, X. *et al.* Adhesion and thermal stability enhancement of IZO films by adding a primer layer on polycarbonate substrate. *physica status solidi (a)* **212,** 831–839, doi: 10.1002/pssa.201431685 (2015).
28. Huang, S., Jiang, Q., Yang, S., Zhou, C. & Chen, K. J. Effective Passivation of AlGaN/GaN HEMTs by ALD-Grown AlN Thin Film. *IEEE Electron Device Letters* **33,** 516–518, doi: 10.1109/LED.2012.2185921 (2012).

Acknowledgements

Author Contributions

H.W. Hou and Z. Liu constructed the original idea and designed the experiments; H.W. Hou carried out experiments and wrote the manuscript; J.H. Teng, T. Palacios and S.J. Chua analyzed the experimental data, discussed the results and revised the manuscript. All authors reviewed the manuscript.

Additional Information

Competing Interests: The authors declare no competing financial interests.

How to cite this article: Hou, H. W. *et al.* High Temperature Terahertz Detectors Realized by a GaN High Electron Mobility Transistor. *Sci. Rep.* **7,** 46664; doi: 10.1038/srep46664 (2017).

Publisher's note: Springer Nature remains neutral with regard to jurisdictional claims in published maps and institutional affiliations.